The Journal of Experimental Biology 207, 2443-2453
Published by The Company of Biologists 2004
doi:10.1242/jeb.01053

Pre-receptor profile of sensory images and primary afferent neuronal representation in the mormyrid electrosensory system

Leonel Gómez[1], Ruben Budelli[1], Kirsty Grant[2] and Angel A. Caputi[3,*]

[1]*Departamento de Biología Celular y Molecular, Facultad de Ciencias, Universidad de la Republica, Montevideo, Uruguay,* [2]*Unité de Neurosciences Intégratives et Computationnelles, CNRS-UPR 2191, Gif sur Yvette, France* and [3]*División de Neurofisiología Comparada (Unidad Asociada a la Facultad de Ciencias, Universidad de la Republica) IIBCE, Montevideo, Uruguay*

*Author for correspondence (e-mail: angel@iibce.edu.uy)

Accepted 27 April 2004

Summary

Afferent responses to the fish's own electric organ discharge were explored in the electrosensory lobe of the mormyrid fish *Gnathonemus petersii*. In order to understand the neural encoding of natural sensory images, responses were examined while objects of different conductivities were placed at different positions along the skin of the fish, i.e. at different points within, and also outside, peripheral receptive fields. The presence of an object in the fish's self-generated electric field produces local modulation of transcutaneous current density. Measurement of the local electric organ discharge shows that object images formed at the electroreceptive sensory surface have an opposing center-surround, 'Mexican hat' profile. This is a pre-receptor phenomenon intrinsic to the physical nature of the sensory stimulus that takes place prior to neural lateral inhibition and is independent of such central inhibition.

Stimulus intensity is encoded in the latency and number of action potentials in the response of primary afferent fibers. It is also reflected in changes in the amplitude and area of extracellular field potentials recorded in the deep granular layer of the electrosensory lobe. Since the object image consists of a redistribution of current density over the receptive surface, its presence is coded by change in the activity of receptors over an area much larger than the skin surface facing the object. We conclude that each receptor encodes information coming from the whole scene in a manner that may seem ambiguous when seen from a single point and that, in order to extract specific object features, the brain must process the electric image represented over the whole sensory surface.

Key words: Mexican hat, electric fish, latency code, electric image, electrolocation, electrosensory lobe, distributed sensory representation.

Introduction

The electric organ discharge (EOD) of weakly electric fish generates transcutaneous electric currents that stimulate electroreceptors distributed over the fish's body surface. The presence of a nearby object whose conductivity is different from that of water produces an electric image consisting of the distortion of the transcutaneous current distribution (Heiligenberg, 1975; Bastian, 1986). Theoretical models (Caputi et al., 1998; Budelli and Caputi, 2000; Sicardi et al., 2000) have suggested two rules for the formation of electric images. Rule 1: objects more conductive than water cause a local increase in transcutaneous current in the region facing the object and a decrease in the transcutaneous current in surrounding regions. Non-conductive objects produce an opposite pattern of modulation. Experimental measurements at the receptive surface confirm this opposing 'center-surround' structure of the projected object image (Caputi et al., 1998; von der Emde et al., 1998). A compatible pattern was described in the primary afferent response by Hagiwara and Morita (1963), Szabo and Hagiwara (1967) and Scheich and Bullock (1974), although its functional importance was recently questioned (Rasnow, 1996; Nelson and McIver, 1999). Rule 2: the electric image spreads and blurs as the distance between the fish and the object increases. This modulation can be quantified as the ratio of the slope of the edge of the projected image to its maximum amplitude (Caputi et al., 1998; von der Emde et al., 1998). Behavioral experiments have shown that this parameter is probably used by mormyrids to discriminate the relative distance of objects (von der Emde et al., 1998).

Mormyromast electroreceptors are innervated by two types of primary afferent fibers (types A and B), which project centrally to different regions of the electrosensory lobe (ELL). Stimulus intensity is related to action potential latency in both types of primary afferents (Bell, 1990a,b), but it has been suggested that type A primary afferents exclusively code stimulus amplitude (von der Emde and Bleckmann, 1992, 1997), while the firing of type B afferents is probably related

to the coding of the waveform of the local electric organ discharge (LEOD), allowing the fish to perceive the impedance-related 'qualia' (Lewis, 1929) of the object (i.e. 'electric color'; von der Emde, 1990; von der Emde and Ronacher, 1994; Budelli and Caputi, 2000).

The present paper deals specifically with the spatial coding of electrosensory images and therefore with primary afferent input arising from Type A mormyromast electroreceptor cells. We tested the following hypotheses: (1) the latency code transmits most of the information about the intensity of the sensory signal; (2) there is distributed coding of object position and other properties at the primary afferent level and (3) the spatial coding pattern of images conforms to the opposing center-surround 'Mexican hat' distribution, as described in previous studies. These issues were explored by recording the LEOD simultaneously with the population field potentials and unitary activity of primary afferents at their terminal region in the granular layer of the ELL, in discharging fish in the presence and absence of stimulus objects.

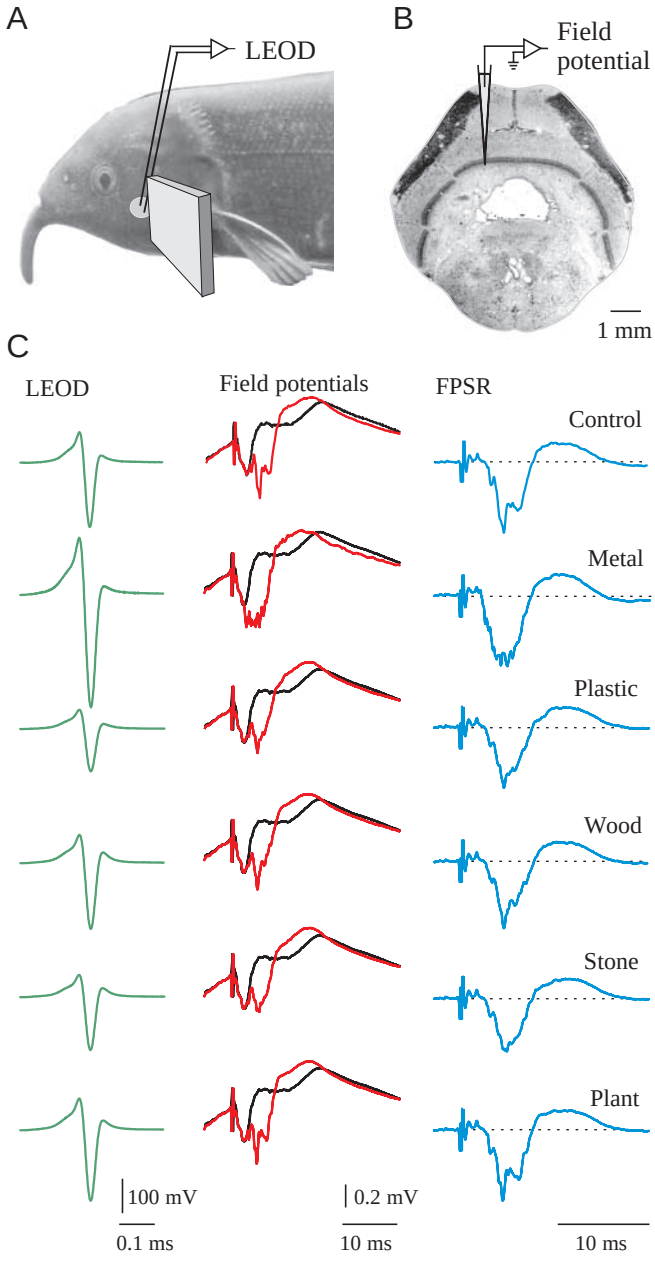

Materials and methods

Ten *Gnathonemus petersii* Günther 1862 were used in this study. The fish were obtained from a registered commercial supplier (Aquarélite, Aufargis, France). They ranged in length from 10 to 14 cm and were probably at the young adult stage. The fish were housed in aquaria representing their natural habitat, in a licensed animal housing facility conforming to national and international standards. Animal care and all experimental procedures were approved by the authors' institutions' animal care and use committees and were carried out in accordance with international guidelines as set out by the European Convention for the Protection of Animals used for Experimental and other Scientific Purposes, the US Public Health Service Policy on Humane Care and Use of Laboratory Animals (PHS Policy) and the National Institutes of Health Guide for the Care and Use of Laboratory Animals (NIH Guide).

Fig. 1A shows the experimental paradigm. Experiments were performed under etomidate anesthesia (Hypnomidate; Janssen-Cilag, Issy les Moulineaux, France; 2 mg l^{-1} for induction, 1 mg l^{-1} during surgery, 450–500 μg l^{-1} during recording, dissolved in aerated water at 22°C, conductivity 170 μS cm^{-1}, perfused through the gills at a rate of 40 ml min^{-1}). Experimental measurement (K. Grant, unpublished observation) has shown that this dose of etomidate does not alter the form or the strength of the natural EOD, although the discharge rhythm is slower and more regular than in the awake state.

The fish's head was immobilized by a plastic rod attached

Fig. 1. (A) Schema of experimental paradigm, showing the object (a metal plate), the receptive field on the skin surface (gray circle) and the position of the electrode pair used to record the local electric organ discharge (LEOD). (B) Photomicrograph of the electrosensory lobe (ELL) in cross section, showing the position of the microelectrode recording field potentials in the granular layer. (C) Comparison of LEODs recorded at the receptive surface and field potentials recorded in the ELL for the control situation without any external object and in the presence of a variety of objects of different conductivity but similar in volume and form, aligned with the center of the receptive field. Left column: LEOD recorded at the receptive field center (green). Middle column: field potentials recorded in the ELL in the presence of a reafferent sensory input (red) and in the absence of reafferent sensory input (black). To obtain the latter traces, the output of the electric organ was shunted with a metal plate close to the tail: in this case reafferent sensory input is absent and the field potential corresponds to the effect of the corollary discharge alone. Right column: the field potential equivalent to the sensory response (FPSR; blue) calculated as the difference between the recordings with and without reafferent input (red minus black traces in middle column). Field potentials are averages of 10 traces.

to the skull, which held only the dorsal surface above the water level in the recording tank. The fish's body was submerged, supported against a sponge with three strands of soft cotton thread (diameter 1 mm). A section of the skull above the ELL was removed and the valvula cerebelli overlying the electrosensory lobe was reflected laterally, to allow visual guidance of electrode placement.

Averaged field potentials (N=10) and unitary activity were recorded from the Type A mormyromast primary afferent terminal region in the granular and intermediate layers of the medial zone of the ELL using glass micropipettes (3 MΩ, filled with 3 mol l^{-1} NaCl, for field potentials; 150–200 MΩ, filled with 2 mol l^{-1} KCH_3SO_4, for intracellular or extracellular unit recordings) connected to a high-input impedance amplifier (Axoclamp 2A; Axon Instruments, Union City, CA, USA) used in Bridge mode. Signals were digitized using a Labmaster interface (Scientific Solutions, Mentor, OH, USA) and processed with a computer running Acquis1 (Gérard Sadoc, C.N.R.S., France) and Matlab (Scientific Solutions) software.

Microelectrodes were positioned using the depth from the surface of the ELL and the characteristic shape of the field potentials as landmark guides (Bell et al., 1992). In two experiments, electrode position in the granular layer was verified by iontophoretic deposit of pontamine sky blue (Hellon, 1971), identified histologically following post-mortem fixation and sectioning. For each electrode track, the cutaneous receptive fields of primary afferent fibers recorded in the granular and intermediate layers of the ELL were identified by applying local electrical stimulation (100 μs constant current square pulses) in the water close to the skin *via* a pair of silver ball electrodes placed 2.5 cm apart, oriented perpendicular to the skin. Sensory responses to the fish's own EOD were then examined in the presence of different types of objects positioned at different distances from the cutaneous receptive field center: (1) aluminum and Teflon cylinders (16 mm diameter, 50 mm length) with the long axis perpendicular to the skin surface; (2) an aluminum plate (3 mm×23 mm×50 mm) with the long axis perpendicular to the skin surface; (3) aquatic plants; (4) a stone and (5) a piece of water-saturated mangrove root. The last three natural objects were similar in volume to the aluminum and Teflon cylinders, although more irregular in shape.

Primary afferent input to the ELL is organized in a topographically ordered manner. EOD-related field potentials recorded in the granular and intermediate layers of the ELL (Fig. 1) are generated by integration of reafferent electrosensory input with a corollary discharge signal driven by the electromotor command (Bell et al., 1992). The modulation of this complex field potential by reafferent electrosensory input (representing the object image) was calculated by subtraction. To make this calculation, reafferent sensory input could be removed in two ways, revealing the electric organ corollary discharge (EOCD) field potential alone. The first method was to inject intramuscularly 100 μg of d-tubocurarine chloride (Sigma, St Louis, MO, USA), which blocked cholinergic neurotransmission between electromotoneurons and the electric organ, thus abolishing the EOD, while the central motor command and the EOCD remained intact. An alternative and reversible block of reafferent sensory input was obtained by short-circuiting the electric organ with a metal plate (3 mm×23 mm×50 mm) placed parallel and very close to the electric organ. The resulting isolated EOCD field potential recorded in the ELL was similar using either of the two methods. A similar procedure in which a plastic plate was placed parallel to the electric organ also allowed us to modulate global field distribution and increase the LEOD in anterior regions of the body, in experiments whose aim was to correlate LEOD amplitude with primary afferent spike timing.

The reafferent electrosensory input could then be calculated by subtraction of the EOCD-alone field potential from the field potential evoked when the EOD was present. We have called this difference the field potential change corresponding to the sensory response (FPSR). Using this measure it was then possible to make quantitative comparison of the neural images of sensory input obtained in the absence of an object (control) and in the presence of any of the objects mentioned above.

In 21 cases we also recorded the effect of objects on the unitary spiking activity of primary afferent fibers. These were identified by their characteristic patterns of discharge consisting of a short-latency (5.5–7 ms) train of two or three spikes rising from the baseline with only small variability for a given stimulus (Bell, 1990a,b).

Natural stimulus intensity at the receptive surfaces was quantified from the LEOD recorded close to the skin, using a pair of steel wire electrodes (exposed tips 1.5 mm long, separated by 2.5 mm). The LEOD signal was recorded with a Tektronix 5A22N differential amplifier in a Tektronix 5223 digital oscilloscope, connected *via* a GPIB interface to a computer running Acquis1 software (Gérard Sadoc, C.N.R.S.). This gave sufficient resolution in A/D conversion to reproduce the rapid signal of the EOD without attenuation or distortion.

Results

The neural response to reafferent electrosensory input was evaluated from the spiking activity of primary afferent fibers, recorded in the deeper layers of the ELL and from the complex field potential that is associated with every EOD. Field potentials in the ELL result from the interaction of descending input, in the form of a corollary discharge signal driven by the electromotor central pattern generator, and re-afferent electrosensory input generated as a result of the EOD.

When an object interferes with the EOD-generated electric field, this causes a change in the basal neural response recorded in the ELL. A maximum change is observed when the object faces the zone of the skin from which primary afferents project to the recorded point of the ELL. Here, we define this region of the skin as the center of the receptive field. The following sections deal with the neural response when (1) the object faces the center of the receptive field and (2) the object position is changed.

The neural response at the center of the receptive field

The left column of Fig. 1C shows LEODs recorded at the center of the peripheral receptive field for five different objects of similar volume and shape but of different materials. The LEOD in the presence of a piece of water-saturated dead wood was similar to the LEOD in the absence of any object (control). The peak-to-peak amplitude of the LEOD was diminished in the presence of the plastic cylinder and the stone and increased in the presence of the living plant and the metal cylinder. These measurements show that the natural stimuli produced by plants, stones or wood fall within the range of those produced by the aluminum and Teflon cylinders used in the experiments described here.

The middle column in Fig. 1C illustrates the field potentials recorded in the ELL granular layer in the presence of the same objects (red traces) and compares them with the field potentials evoked at the same recording site by the corollary discharge input alone (black traces) when the EOD and the consequent reafferent input had been blocked by shunting the EOD with a metal plate placed parallel to the body very close to the electric organ. The contribution of the reafferent sensory input can be calculated as the difference between these traces, illustrated in the right column of Fig. 1C (FPSR).

Despite the differences in object characteristics, all the FPSR traces had an initial sharp negative wave followed by a broader positive wave. An increment in LEOD amplitude was associated with reduced latency and increased amplitude of the early sharp negative wave of the FPSR (e.g. compare traces for metal and plastic objects in Fig. 1C). Reductions in LEOD amplitude were associated with opposite changes in the FPSR.

The FPSR is, however, a complex response that corresponds to the activity of primary afferent input as well as several different types of neurons of the ELL excited by the afferent input in the presence of the corollary discharge signal. Records of spiking activity show that reafferent primary electrosensory input arrives in the ELL 5–12 ms after the beginning of spinal electromotoneuron activity (i.e. 2–9 ms after the EOD whose artifact can be observed in the records), corresponding to the early negative component of the FPSR. The results described below focus on the early processing of the reafferent sensory image and therefore will deal only with this part of the FPSR. The later positive wave of the FPSR represents later stages of activity in the intrinsic network, which will be the subject of future publication.

Change in amplitude of the LEOD causes changes in the amplitude, number and latency of the multiple peaks of the field potential response produced by the activity of a population of afferent fibers. Larger LEODs reduce the latency and increase the number of primary afferent action potentials and also increase the probability that more fibers fire at the same time. As a consequence, the negative peak of the field potential starts earlier and increases in area. Thus, the early negative component of the FPSR is also a sensitive index by which to estimate primary afferent activity.

In order to study the relationship between LEOD amplitude and FPSR modulation in greater detail, the amplitude of the LEOD was modified by placing a large metal plate in the tail region, orientated parasagittally, first close to the electric organ and then at different distances lateral to the fish's tail (Fig. 2A). Close to the electric organ, this produces a large reduction in external resistance, equivalent to a local short-circuit at the current source. The consequence is a redistribution of currents within the global field: the fraction of current flowing into the anterior regions of the fish's body is reduced, and in this case the rostral part of the body is in the 'surround' region of the Mexican hat. As the plate is moved further away from the tail, the local short-circuit effect at the current source diminishes and the metal plate starts to behave as any conductive object placed far away. With increasing distance between the metal plate and the electric organ, the object image becomes wider (see Fig. 6), and at a distance of several centimeters the whole ipsilateral surface of the fish falls within the central region of the Mexican hat, producing an increase in the current flowing through the whole ipsilateral receptive surface. A plastic plate close to the tail produced opposite effects. Fig. 2A illustrates the changes in the FPSR as the LEOD amplitude was modulated in this manner.

The peak amplitude of the early negative wave of the FPSR was related to the LEOD amplitude but was a 'noisy' measure of this variable due to underlying spike activity. The area of the early negative peak of the FPSR was highly correlated with the LEOD amplitude (Fig. 2A, r^2= 0.99, P<0.01, N=36). It was also a highly correlated decreasing function of the FPSR latency measured at 50% amplitude (Fig. 2B). The inter-dependence of these parameters suggests that each one codes the LEOD peak-to-peak amplitude and that the other parameters do not add extra information.

The area and the latency of the early negative peak of the FPSR are also related to the latency and the number of spikes of the primary afferent unitary response. Extracellular or intracellular records of unit activity examined as a function of LEOD amplitude confirmed observations made using artificial stimuli. As stimulus intensity is increased, the latency of the first spike of the response is reduced and the number of spikes in the response burst increases (Szabo and Hagiwara, 1967; Bell, 1990b; von der Emde and Bleckmann, 1992).

Fig. 2C shows a raster diagram of spike timing for a single afferent fiber recorded as a metal object was moved steadily along the body, passing across the receptive field. The latency of the first spike reached its minimum at the center of the receptive field (zero on the ordinate) and changed smoothly with object position on either side of that point. In addition, the interval between the first and second spikes was a precise function of the latency of the first spike (Fig. 2D), showing that the timing of the second spike is predictable from the latency of the first one. These observations strengthen the interpretation that a single parameter, probably peak-to-peak amplitude of the LEOD, is coded by the latency of the primary afferent spike train (Bell et al., 1992) and similarly by the area or latency of the negative peak of the sensory field potential.

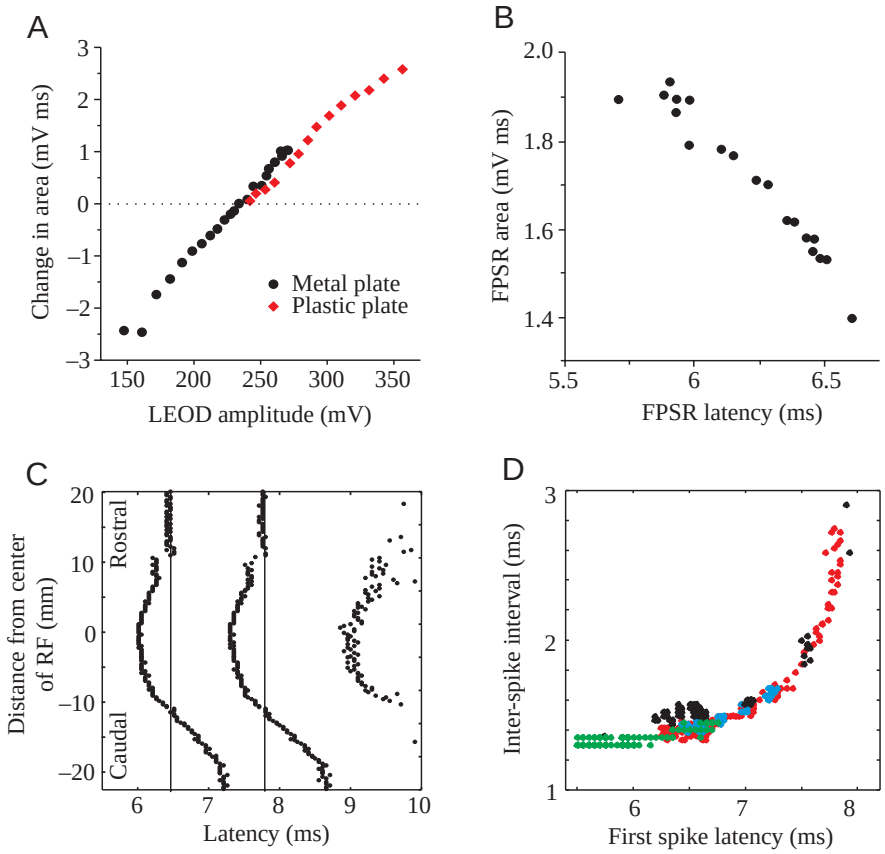

Fig. 2. Electrosensory coding by field potentials and primary afferent unit activity. (A) Change in area of the negative peak of the field potential equivalent to the sensory response (FPSR) plotted as a function of the peak-to-peak amplitude of the local electric organ discharge (LEOD), when a metal plate (black circles) or plastic plate (red diamonds) were placed parallel to the fish in the region of the electric organ, at increasing distances lateral to the fish's body. Zero represents the control value, in the absence of any object. (B) Area of the negative peak of the FPSR as a function of its latency at half-amplitude. (C) Raster plot of the activity of a single afferent fiber while a metal object was moved along the side of the fish. The vertical lines indicate the mean latencies of spike timing in the absence of any object (two spikes only). (D) Interval between the first and the second spikes as a function of the latency of the first spike after the motor command. Points of different colors correspond to data from different primary afferent units recorded in the same fish.

Sensory responses as a function of the position of the object

The increasing relationship between the LEOD amplitude and responses recorded in the ELL suggests strongly that the opposing 'center-surround' (Caputi et al., 1998; von der Emde et al., 1998) structure of the object image projected on the sensory surface is conserved in the response of primary afferents.

To go further in understanding how the sensory image is formed, it is first necessary to know how the stimulus driving the afferents projecting to the recording region changes with the position of the object. Instead of recording the complete set of responses at different points of the ELL, we took the alternative step of recording at a single point in the ELL as an object was moved in successive steps past the center of the receptive field. Fig. 3 shows schematically the expected stimulus variations in the case of a metal object. Because the energy source for the stimulus is located caudally (i.e. at the electric organ), the Mexican hat profile of the sensory image is asymmetric, with a deeper trough on the rostral front. This means that the contrast is greater at the rostral border of the image. Thus, when a metal object is situated caudally to the center of the receptive field (Fig. 3A, red), the electroreceptors will see the deep rostral trough of the Mexican hat image profile (Fig. 3B, red trace), where the LEOD is significantly decreased compared with the basal value (Fig. 3C, red dot). When the object is rostral to the center of the receptive field (Fig. 3A, blue), the center of the receptive field will see the more shallow caudal trough of the image profile (Fig. 3B, blue trace) producing a relatively smaller surround effect (Fig. 3C, blue dot).

The local electric field generated by the EOD decays with distance from the tail towards the head. The spatial attenuation of this decay depends on the relative conductivity of the water and the internal fish tissues (for any given experiment this was constant). Because of this caudal-to-rostral decay of the electric field generated by the EOD (the signal carrier), the image of a given object is less intense when it is situated towards the head of the fish (Fig. 3B, blue line) than when it is located caudally (Fig. 3B, red line). This effect increases still further the difference between the rostral trough of a caudal object image and the caudal trough of a rostral object image (compare red and blue dots in Fig. 3C). As shown in the graph of Fig. 3C, the net dynamic effect seen at the receptive field as an object moves past is also a Mexican hat profile but is a 'mirror' image of the stationary object image. The asymmetry of the image is increased and the surround effect is greater at the caudal margin than at the rostral edge. In mathematical terms, as an object moves from caudal to rostral, passing through the receptive field, the dynamic record obtained at a given point in the electrosensory network is the convolution of the basal local EOD (the signal carrier) and the asymmetrical Mexican hat profile of the electric image (the signal).

Fig. 4 illustrates the progress of the FPSR early negative peak as conducting and non-conducting objects are moved

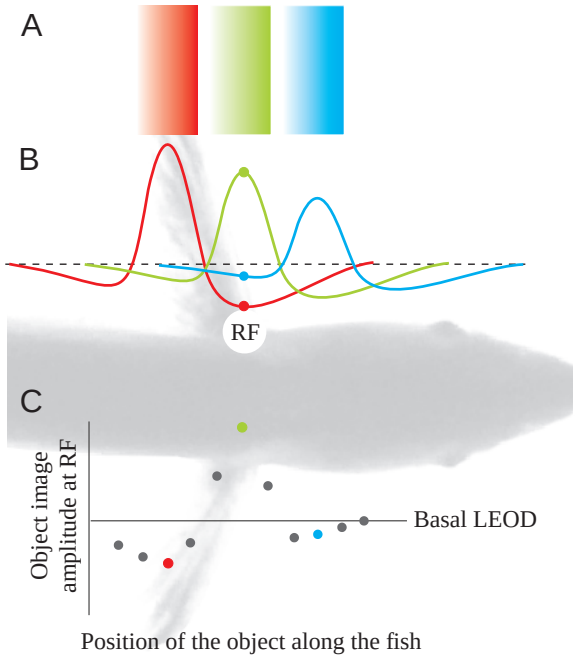

Fig. 3. This theoretical schema explains qualitatively how the local electric organ discharge (LEOD) at the receptive field center (RF) changes with the position of a conductive object. (A) The colored bars indicate different positions of a cylindrical object. (B) Colored curves indicate the corresponding image profile, i.e. the change in LEOD peak-to-peak amplitude compared with the basal LEOD (broken line), projected on the fish's receptive surface when the object is placed at the different positions indicated by corresponding colors in A. Image amplitudes at points indicated by colored dots are plotted below in C. (C) The changing image as the object moves past the receptive field center. The graph was constructed by plotting the change in LEOD peak-to-peak amplitude seen at the center of the receptive field as a function of the rostro-caudal position of the object. Colored points represent the image amplitude compared with the basal LEOD, seen at the receptive field center when the object is in the corresponding color-coded position. Note that this graph reflects the Mexican hat shape present in the LEOD profiles but shows inverse asymmetry: thus, when the object is caudal to the center of the receptive field, the surround effect at the receptive field center is larger than when the object is rostral.

from rostral to caudal through the center of the receptive field, following the body profile at a distance of 2 mm from the skin. Metal and plastic cylindrical objects produced opposite modulation of the field potentials recorded in the ELL. A peak modulation of the FPSR early negative wave was found when the center of the object was at the center of the cutaneous receptive field (Fig. 4, gray bar at position 0 mm). Rostral to the receptive field center, the modulation of the sensory response decayed to close to the control situation. When the object was caudal to the cutaneous receptive field, the modulation of the sensory response was opposite to that observed when the object was in line with the center of the cutaneous receptive field.

Plastic objects produced a relatively smaller, spatially narrower modulation of the sensory response than metal objects. These results fit with previous simulations, predicting that metal objects would produce a larger modulation of the LEOD than plastic objects (Sicardi et al., 2000). This asymmetry of the images formed by conductive and non-conductive objects is because the difference between the conductivity of the plastic and the water is much smaller than the difference between the metal and the water. In addition, the asymmetry of the images formed by conductive and non-conductive objects is enhanced because the strength of the source equivalent to the field distortion produced by the object is non-linearly dependent on object conductivity.

It is also interesting to note that the curves for plastic and metal objects have a different shape when the object is in the caudal region of the fish's body. Here, a metal object produces increasing attenuation as it moves closer to the electric organ source. This is because a metal object short-circuits the electric organ output, significantly reducing the sensory stimulus in all rostral regions. In the extreme case when a large metal object is exactly aligned with the electric organ, reafferent sensory input is absent and the field potential recorded in the ELL is similar to that generated by the EOCD alone, for instance recorded in a curarized fish in the absence of an EOD.

Fig. 5 illustrates this Mexican hat phenomenon coded in the primary afferent firing pattern (top) and field potential color maps (bottom). The two upper raster diagrams show the timing of action potentials fired by a single primary afferent fiber in response to the EOD, when a plastic object and a metal object were positioned at 10 successive points passing through the center of the cutaneous receptive field.

The primary afferent fiber fired two or three action potentials, depending on the nature of the object (plastic or metal) and its location relative to the receptive field center. For a metal object, the latency of the first spike was shortest when it was positioned in the center of the receptive field (ordinate 0 mm). When the metal object was either caudal or rostral to

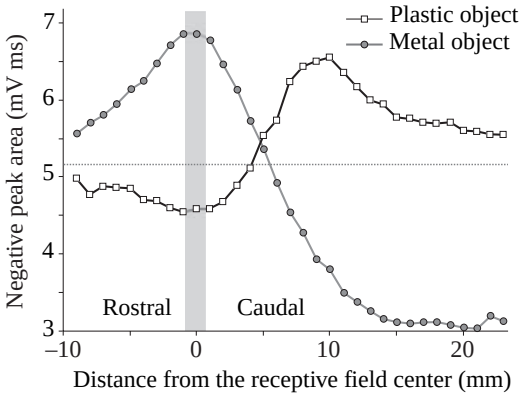

Fig. 4. Area of the field potential equivalent to the sensory response (FPSR) negative peak as a cylindrical object (metal or plastic, oriented perpendicular to the skin) was moved from rostral to caudal along the body, passing through the center of the receptive field (gray bar, 0 mm). The horizontal dotted line indicates the area of the FPSR negative peak in the absence of any object, as a control value.

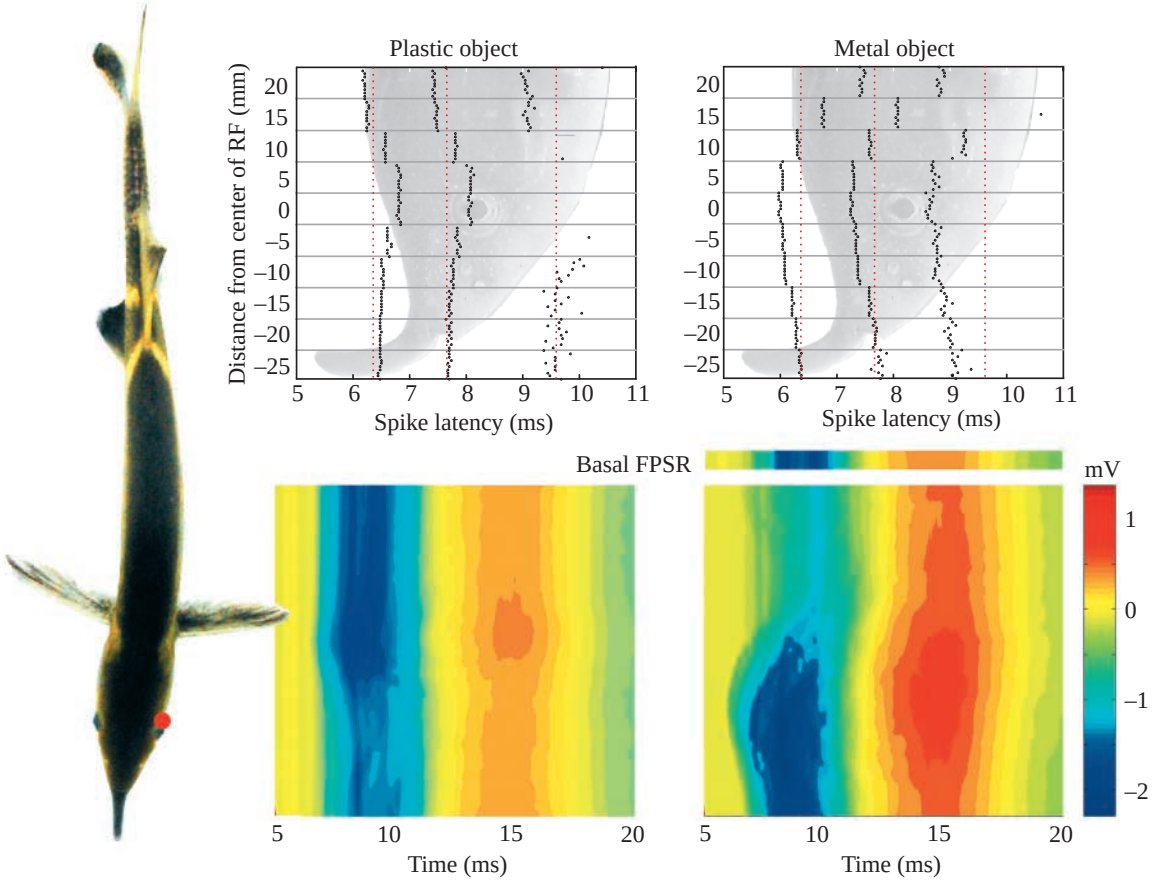

Fig. 5. Primary afferent and field potential response patterns to objects of different conductivity. Top: primary afferent unitary response as a function of the longitudinal position and conductivity of the object. Two groups of 10 raster diagrams show the latency of a primary afferent unit firing when a plastic object (left) or a metal object (right) was moved in 5 mm steps along the fish's body. Position zero indicates the center of the receptive field. Bottom: the color maps represent the field potential equivalent to the sensory response (FPSR) as a function of time after the electromotor command (horizontal axis) and as a function of object position along the fish's body, relative to the receptive field center (red dot; vertical axis indicated by the fish body at the left). Results obtained with a plastic cylinder are shown on the left and with a metal cylinder on the right. The horizontal color bar shows the basal FPSR in the absence of an object. The vertical color bar indicates the color code for instantaneous voltage of FPSR record. (Note that the time scales used in the raster plots and the color maps are different.)

the receptive field center, the latency of the primary afferent action potentials was longer and the variability of the timing of the second and third action potentials of the train increased. At 15 mm caudal to the receptive field center, the third action potential dropped out of the response. In the presence of the plastic object, the latency of primary afferent action potentials varied in an opposite manner. Latency was longest when the plastic object was in line with the receptive field center, and here the EOD evoked only two action potentials. In each series, the timing of the three action potentials evoked by the EOD in the absence of any object is shown by the dotted red lines. It can be seen that in both cases the effect of the object on action potential timing inverted between 10 and 15 mm caudal to the receptive field center and that this effect was larger for the metal object.

These results confirm the findings of earlier work in mormyrids (Szabo and Hagiwara, 1967) and in gymnotid electric fish (Hagiwara and Morita, 1963; Scheich and Bullock, 1974; Bastian, 1981a,b) that showed that, for individual afferent fibers, the latency of spikes generated when a conductive stimulus object was present in the surround region of the receptive field was greater than latencies of spikes generated by the EOD alone in the absence of any object. Here, we have demonstrated how both highly conductive and poorly conductive objects modulate the reafferent sensory response to the EOD, in a manner that is compatible with the Mexican hat profile of the object image, and produce effects of opposite sign depending on object conductivity.

The lower panels of Fig. 5 show field potential responses as a function of object position along the fish. [This section uses a different time scale, showing the period from 5 to 20 ms following the firing of the electromotoneurons (conventional 0 of the system).] The horizontal axis indicates time, while the vertical axis shows the position of the object relative to the fish's body illustrated on the left; voltage above or below zero is color coded, as shown in the vertical calibration bar to the

right. The basal field potential response recorded in the absence of objects is shown as a separate strip at the top. These field potential diagrams show darker blue regions indicating the negative peaks in the response. The red region indicates the slow positive wave that follows the negative peak (see Fig. 1). For a metal cylinder (right), the blue region increased in size and decreased in latency when the conductive object moved towards the center of the receptive field. The opposite pattern was seen for a plastic cylinder in different positions relative to the center of the receptive field (left).

To address how sensory responses depend on the distance between the fish and the object, we repeated the experimental protocol of Fig. 5, placing a metal object at successive rostro-caudal positions, making several passes through the receptive field at different distances lateral to the skin (Fig. 6). In this case, we used a metal plate oriented perpendicular to the skin surface, whose profile was narrower than the face of the cylindrical objects, in order to generate a sharper object image. In the upper section of Fig. 6, rasters of single primary afferent spike timing show the modulation of the pattern of discharge when the metal plate was moved along the fish's body in sequential 5 mm steps, first at 2 mm from the skin (left) and then at a lateral distance of 7 mm (right). Close to the fish's body, the effect of the object was greater in amplitude and more sharply contrasted than when the object was further away. This is also illustrated in field potential responses, shown in color maps in Fig. 6 (bottom) as the same object was moved along the fish's body at distances of 1, 7 and 17 mm from the skin. As the distance between the object and the fish was increased, the changes in reafferent responses decreased in intensity. The width of the sensory image also increased with distance and the image became more blurred, in agreement with previous theoretical predictions (Caputi et al., 1998; Budelli and Caputi, 2000).

These results indicate that both the primary afferent spiking response and the (more complex) field potential records from the granular layer of ELL are related directly to the local modulation of the EOD seen at the receptive surface in the presence of an object and code the center surround profile of the object image.

However, when recording centrally, it is possible that lateral inhibition might also be involved in the Mexican hat effect observed in the FPSR. Previous experimental studies have shown that the neural phenomenon of lateral inhibition does indeed exist in the electrosensory lobe (Bell et al., 1997; Meek et al., 2001). The experiment illustrated in Fig. 7 was carried out in order to distinguish the effects of the Mexican hat profile of the stimulus from effects due potentially to lateral inhibition. First, an artificial electric stimulus (100 μs pulse) was applied synchronously with the EOD, at points rostral or caudal to the

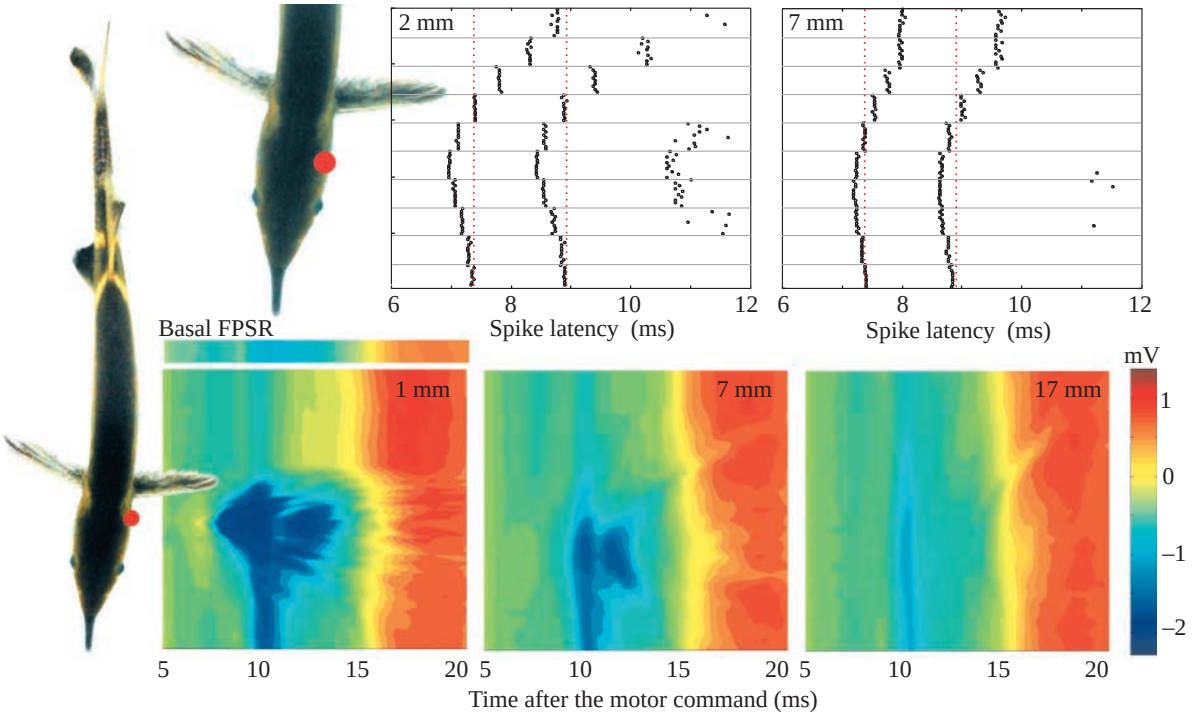

Fig. 6. Response patterns to a metal object located at different distances lateral to the fish's body. Top: primary afferent unit response as a function of the rostro-caudal position and lateral distance of the object. Two groups of 10 raster diagrams represent the latency of the spikes of a primary afferent unit when an object was moved in 5 mm steps rostro-caudally along the fish body, at distances of 2 mm (left) and 7 mm (right) from the skin. The vertical red lines indicate the mean latencies of the basal spike discharges in the absence of an object. Bottom: color maps represent the field potential equivalent to the sensory response (FPSR) as a function of time and object position as in Fig. 5, for objects moved rostro-cadally along the fish's body axis, at lateral distances of 1 mm (left), 7 mm (middle) and 17 mm (right) from the skin. Object position is shown relative to the fish picture on the left; the red dot indicates the receptive field center.

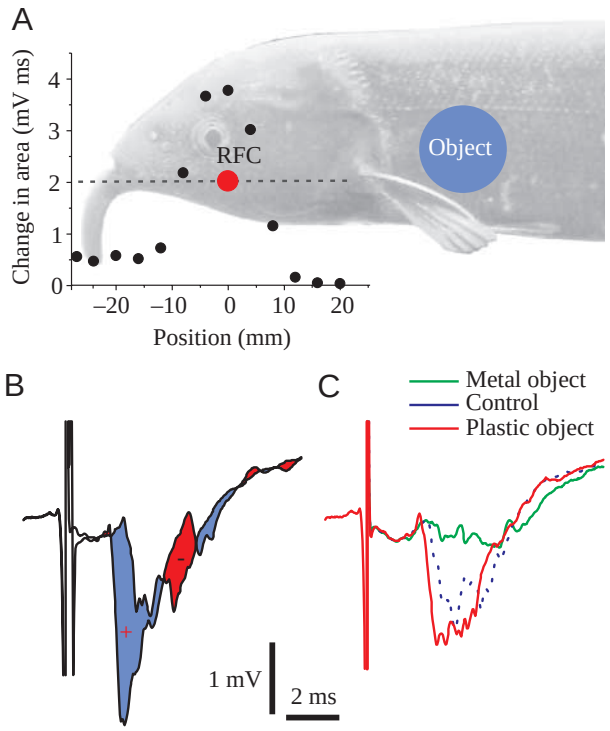

Fig. 7. Effect of the surround on the field potential equivalent to the sensory response (FPSR). (A) An artificial stimulus was given *via* a dipole electrode simultaneously with the electric organ discharge (EOD) at the receptive field center (RFC; red dot; 0 on the horizontal axis of the graph) and at different points along the rostro-caudal axis (dotted line), illustrated relative to the fish's head. Potentiation of the field potential reafferent sensory response (relative to the basal response, =0) was maximal when the simultaneous artificial stimulation was applied close to the receptive field center but was also observed when the artificial stimulation was rostral to the receptive field center or up to 20 mm caudal to this point. Surround inhibition was not seen when the artificial and natural stimuli occurred simultaneously. (B) Comparison of the basal FPSR with that obtained when an artificial excitatory stimulus was applied synchronously with the EOD, in the center of the receptive field. The effect of this stimulus is represented by difference between the two FPSRs, shown by the blue and red areas. (C) The basal FPSR (blue trace; control) and FPSRs obtained at the same recording point when a metal cylinder (green trace) or a plastic cylinder (red trace) were placed facing the non-electroreceptive area of the flank labeled 'object' in A. Electrical stimulation at the same point had no visible effect on the reafferent sensory response.

center of the receptive field (Fig. 7A). This resulted in facilitation of the reafferent sensory response evoked by the EOD when the stimulus was applied from 25 mm rostral up to 10 mm caudal to the center of the receptive field. Fig. 7B illustrates (in blue and red) the difference between the facilitated response and the basal reafferent sensory response at the center of the receptive field. The plot in Fig. 7A shows this effect as a function of the distance to the center of the electric field. When the additional stimulus was applied at a distance greater than 10 mm caudal to the receptive field center, there was no change in the reafferent sensory response. This shows the extent over which excitatory input from the surround region can facilitate the neuronal response in the granular layer of the ELL. Surround inhibition was not seen in these experiments when the additional artificial stimulus and the EOD were synchronous. However, lateral inhibitory interactions have been observed in other experiments using curarized preparations, applying two artificial stimuli: lateral inhibition appears most clearly when using non-synchronous stimulation paradigms, where the conditioning stimulus precedes the test stimulus by at least 2 ms (Kröther et al., 2001).

Next, either a metal or a plastic object (cylinder) was placed 40 mm caudal to the center of the receptive field, facing an area of skin on the fish's lateral flank that bears no electroreceptors (see position in Fig. 7A). In the presence of a metal object, the reafferent sensory response was nevertheless dramatically reduced (Fig. 7C). Since the object was facing skin lacking electroreceptors, this effect could not have been due to inhibition originating from the area immediately facing the metal object. It was more likely due to the surround effect intrinsic to the Mexican hat physical profile of the object image itself. Similarly, when presenting a plastic object at the same position 40 mm caudal to the receptive field center, the latency of the reafferent response decreased and the amplitude of the FPSR increased (Fig. 7C), indicating a stronger stimulus at the center of the receptive field. These results again corroborate the Mexican hat effect as a purely pre-receptor phenomenon. They do not exclude, however, that lateral inhibition probably plays an additional role in sharpening receptive field properties of neurons in the central nervous system, and this will be explored fully in future experiments.

Discussion

Latency codes in primary afferent activity

The present study has shown that objects in the nearby environment modify both the activity of single afferent fibers and the field potentials recorded in the granular layer of the electrosensory lobe. We confirm that the latency, frequency and number of action potentials in single primary afferent discharges all code the amplitude of the LEOD. This was shown here for reafferent electrosensory input evoked by the fish's own EOD in the presence of real object images, rather than the artificial electric stimuli used by earlier authors (Szabo and Hagiwara, 1967; Bell, 1990a,b; von der Emde and Bleckmann, 1992, 1997).

However, our results show that all three of these parameters encode the same variable of the object image, raising the question of why it should be useful to have such signal redundancy. The latency of the first spike of the primary afferent response is closely related to the intervals between this and subsequent spikes of the response, and both are tightly dependent on LEOD amplitude. It has been suggested that the gate created by EOCD-generated excitatory input to granule cells is critical for reading the timing of the first spike of the

reafferent train (Bell, 1986; Gómez, 2001). As the latency of the first spike diminishes, it approaches the peak of the excitatory post-synaptic potential (EPSP) produced by the EOCD in the granule cells. This facilitates the responses of the granule cells, in this way amplifying the reafferent input. If more than one granule cell spike is needed to drive the next postsynaptic neuron, as for example in the case of the proposed ephaptic interactions with large myelinated inhibitory interneurons (Han et al., 2000; Meek et al., 2001) or the deep granular layer large fusiform cells (Meek et al., 2004), the number and frequency of spikes might be important. This speculation suggests how an apparently redundant mechanism of coding may be important in sensory integration in the ELL: different neurons of the intrinsic network of the ELL may extract and address the same information using different information codes.

Distributed nature of electrosensory image processing

Here, we provide evidence that there is a distributed coding of electrosensory images in the early stages of electroreception. Recorded responses of primary afferent activity and field potentials in the ELL indicate that this is based on the Mexican hat pattern intrinsic to the nature of the stimulus, enhanced by the difference between the conductivities of the fish body and the water and probably further shaped by lateral inhibitory neuronal mechanisms in the primary afferent projections and granule cell layer and the interaction with the EOCD.

A common reference for the study and design of image processing mechanisms is mammalian vision. In this sensory system, all points along the same line passing through the optical center of the eye are mapped on a single point of the retina. By the same reasoning, different points of the retina receive information from different zones of space. Thus, we can say that in such a system the physical image results from the apposition of different independent stimuli.

The case for electroreception is different because the finite source of energy is contained within the fish's body. An elementary point object modulates current distribution with a center-surround opposition pattern and distorts the entire electric field. This gives contrast at the level of the sensory surface itself, and the information generated by the elementary object (a single point in space) is contained not only in input from the skin receptors facing the object but also in the overall pattern of transcutaneous current perceived over the whole sensory surface. This phenomenon describes a physical property intrinsic to the nature of the electrosensory stimulus. Such 'distributed' imaging procedures are also present in some other sensory systems (Coombs et al., 1996, 2002). Here, we have confirmed the theoretical prediction that the Mexican hat effect present at the physical image is translated at the primary afferent level and is therefore significant for the electrosensory system. Both physical measurements (Caputi et al., 1998) and theoretical simulation (Sicardi et al., 2000) indicate that the relative slope (slope/maximum amplitude) of the object image varies little with size and conductance of the object and is thus the best indicator of object distance. For example, the latency of the first action potential of the primary afferent response (Fig. 6) increases with the distance of a metal object from the center of the receptive field. Thus, as for the physical object image, the neural response pattern spreads out with distance from the fish's body. Despite the differences between patterns of response to metal and plastic objects, similarities in the relative slopes of their Mexican hat profiles are preserved in the neural response at the primary afferent level. This provides additional support to the hypothesis that fish discriminate object distance by measuring the relative slope of the sensory image (Caputi et al., 1998; von der Emde et al., 1998; von der Emde, 1999).

We also found that in the case of metal objects, the center-surround contrast observed at the primary afferent level is much larger than that at the skin. This is in part due to the asymmetry of the afferent response, caused by the hyperbolic relationship between stimulus amplitude and afferent spike latency (Bell, 1989): reductions in the LEOD result in larger changes in latency (and even failure to produce afferent firing) than corresponding increases in the LEOD. It should also be noted that the spatial profile produced by objects that were similar in shape but of different conductivities were not exact mirror images. For metal objects, the surround response observed centrally at the afferent terminal site is relatively enhanced, but for plastic objects the same hyperbolic relationship tends to diminish the surround effect centrally.

Conclusions

The Mexican hat profile of the stimulus is a physical property of the object image at the level of the receptors and is separate and different from neural lateral inhibition. Because the electric organ is a discrete, finite source located in the fish's body, objects in the nearby environment will always project an image with a center-surround structure, whatever their size. This is because conducting objects locally facilitate the flow of current, with the corresponding subtraction of current from the surrounding region. Plastic objects produce the opposite effect. Because the conductivity of the fish's body is higher than that of water, the opposing center-surround pattern is enhanced, and contrast is locally increased, at the electroreceptive surface. This stimulation pattern is preserved in the primary afferent activity, encoded in the hyperbolic stimulus intensity *versus* spike latency response pattern described by Szabo and Hagiwara (1967) and Bell (1990a). In the presence of an object, the latency of primary afferents firing is decreased or increased with respect to the set-point corresponding to the unperturbed electric field. This is functionally significant since latencies vary within the non-linear gate created by the corollary discharge (Bell, 1989). As a function of this gating mechanism, advances or delays of primary afferent activity produce different responses in the principal cells of the ELL (Gómez, 2001; L. Gómez et al., personal observations).

We thank Drs Thierry Bal, Yves Frégnac and Michael Rudolph for critical reading and useful comments on this manuscript. Work was partially supported by the European

Commission (CI1*-CT92-0085 and IST-2001-34712), an ECOS grant (U97B03) to K.G. and R.B. and a grant from the CSIC – Universidad de la República, Uruguay to A.C. and R.B.

References

Bastian, J. (1981a). Electrolocation I. How the electroreceptors of *Apteronotus albifrons* code for moving objects and other electrical stimuli. *J. Comp. Physiol.* **144**, 465-479.

Bastian, J. (1981b). Electrolocation II. The effects of moving objects and other electrical stimuli on the activities of two categories of posterior lateral line lobe cells in *Apteronotus albifrons*. *J. Comp. Physiol.* **144**, 481-494.

Bastian, J. (1986). Gain control in the electrosensory system mediated by descending inputs to the electrosensory lateral line lobe. *J. Neurosci.* **6**, 553-562.

Bell, C. C. (1986). Duration of plastic change in a modifiable efference copy. *Brain Res.* **369**, 29-36.

Bell, C. C. (1989). Sensory coding and corollary discharge effects in mormyrid electric fish. *J. Exp. Biol.* **146**, 229-253.

Bell, C. C. (1990a). Mormyromast electroreceptor organs and their afferent fibers in mormyrid fish. II. Intra-axonal recordings show initial stages of central processing. *J. Neurophysiol.* **63**, 303-318.

Bell, C. C. (1990b). Mormyromast electroreceptor organs and their afferent fibers in mormyrid fish. III. Physiological differences between two morphological types of fibers. *J. Neurophysiol.* **63**, 319-332.

Bell, C. C., Grant, K. and Serrier, J. (1992). Sensory processing and corollary discharge effects in the mormyromast regions of the mormyrid electrosensory lobe. I. Field potentials, cellular activity in associated structures. *J. Neurophysiol.* **68**, 843-858.

Bell, C. C., Caputi, A. and Grant, K. (1997). Physiology and plasticity of morphologically identified cells in the mormyrid electrosensory lobe. *J. Neurosci.* **17**, 6409-6423.

Budelli, R. and Caputi, A. (2000). The electrical image in weakly electric fish, perception of complex impedance objects. *J. Exp. Biol.* **203**, 481-492.

Caputi, A., Budelli, R., Grant, K. and Bell, C. (1998). The electric image in weakly electric fish, II. Physical images of resistive objects in *Gnathonemus petersii*. *J. Exp. Biol.* **201**, 2115-2128.

Coombs, S., Hastings, M. and Finneran, J. (1996). Measuring and modeling lateral line excitation patterns to changing dipole source locations. *J. Comp. Physiol. A* **178**, 359-371.

Coombs, S., New, J. G. and Nelson, M. (2002). Information-processing demands in electrosensory and mechanosensory lateral line systems. *J. Physiol. Paris* **96**, 341-354.

Gómez, L. (2001). Codificación y procesamiento de la imagen eléctrica en *Gnathonemus petersii*. PhD thesis, PEDECIBA, Uruguay.

Han, V., Grant, K. and Bell, C. C. (2000). Rapid activation of GABAergic interneurons and evidence for calcium-independent release of GABA in the mormyrid electrosensory lobe. *J. Neurophysiol.* **83**, 1592-1604.

Hagiwara, S. and Morita, H. (1963). Coding mechanisms of electroreceptor fibers in some electric fish. *J. Neurophysiol.* **26**, 551-567.

Heiligenberg, W. (1975). Theoretical and experimental approaches to spatial aspects of electrolocation. *J. Comp. Physiol.* **103**, 247-272.

Hellon, R. F. (1971). The marking of electrode tip positions in nervous tissue. *J. Physiol.* **214**, 12P.

Kröther, S., Engelman, J., von der Emde, G., Bleckmann, H. and Grant, K. (2001). Spatial and temporal structuring of lateral inhibition and convergent summation in encoding electrosensory images. In *Göttingen Neurobiology Report 2001* (ed. N. Eisner and G. W. Kreutzberg), p. 444. Stuttgart, Germany: Georg Thieme Verlag.

Lewis, C. I. (1929). *Mind and the World Order*. New York: C. Scribner's Sons.

Meek, J., Hafmans, T. G. M., Han, V., Bell, C. C. and Grant, K. (2001). Myelinated dendrites in the mormyrid electrosensory lobe. *J. Comp. Neurol.* **431**, 255-275.

Meek, J., Kirchberg, G., Grant, K. and von der Emde, G. (2004). Dye coupling without gap junctions suggests excitatory connections of gamma-aminobutyric acidergic neurons. *J. Comp. Neurol.* **468**, 151-164.

Nelson, M. and McIver, M. (1999). Prey capture in the weakly electric fish *Apteronotus albifroms*, Sensory acquisition strategies and electrosensory consequences. *J. Exp. Biol.* **202**, 1195-1203.

Rasnow, B. (1996). The effects of simple objects on the electric field of *Apteronotus Leptorhynchus*. *J. Comp. Physiol. A* **178**, 397-411.

Scheich, H. and Bullock, T. H. (1974). The detection of electric fields from electric organs. In *Handbook of Sensory Physiology* (ed. A. Fessard), pp. 201-256. Berlin: Springer-Verlag.

Sicardi, E. A., Caputi, A. and Budelli, R. (2000). Physical basis of distance discrimination in weakly electric fish. *Physica A* **283**, 86-93.

Szabo, T. and Hagiwara, S. (1967). A latency-change mechanism involved in sensory coding of electric fish (mormyrids). *Physiol. Behav.* **2**, 331-335.

von der Emde, G. (1990). Discrimination of objects through electrolocation in the weakly electric fish, *Gnathonemus petersii*. *J. Comp. Physiol. A* **167**, 413-421.

von der Emde, G. (1999). Orientation in the dark, brain circuits involved in the perception of electric signals in mormyrid electric fish. *Eur. J. Morphol.* **37**, 200-205.

von der Emde, G. and Bleckmann, H. (1992). Differential responses of two types of electroreceptive afferents to signal distortions may permit capacitance measurements in a weakly electric fish, *Gnathonemus petersii*. *J. Comp. Physiol. A* **171**, 683-694.

von der Emde, G. and Bleckmann, H. (1997). Waveform tuning of electroreceptors cells in the weakly electric fish, *Gnathonemus petersii*. *J. Comp. Physiol. A* **171**, 683-694.

von der Emde, G. and Ronacher, B. (1994). Perception of electric properties of objects in weakly electric fish, two-dimensional similarity scaling reveals a City-Block metric. *J. Comp. Physiol. A* **175**, 801-812.

von der Emde, G., Schwarz, S., Gómez, L., Budelli, R. and Grant, K. (1998). Electric fish measure distance in the dark. *Nature* **395**, 890-894.